Analyst

PAPER

View Article Online
View Journal | View Issue

Cite this: *Analyst*, 2019, **144**, 4781

Bottom-up and top-down profiling of pentosan polysulfate

Lei Lin,†[a] Yanlei Yu,†[b] Fuming Zhang,[c] Ke Xia,[b] Xing Zhang*[d,e] and Robert J. Linhardt *[b,c]

Pentosan polysulfate (PPS) is a semi-synthetic glycosaminoglycan (GAG) mimetic. PPS, synthesized through the chemical sulfonation of a plant-derived β-(1 → 4)-xylan, is the active pharmaceutical ingredient of the drug Elmiron™ used to treat interstitial cystitis. Unlike natural GAGs that can be enzymatically broken down into oligosaccharides for analysis, PPS is an unnatural polyanionic polysaccharide and is not amenable to such an analytical approach. Instead reactive oxygen species were used for the controlled depolymerization of PPS and the resulting oligosaccharide fragments were then analyzed by liquid chromatography-mass spectrometry (LC-MS) to obtain bottom-up information on its composition. Because PPS has an average molecular weight ranging from 4000 to 6000 Da, similar to that of low molecular weight heparin, this suggested that it might be possible to use LC-MS on its intact chains and perform top-down analysis. The bottom-up and top-down analysis of PPS provides the first detailed compositional and structural information on PPS. Finally, we examined whether PPS would interfere with polysaccharide lyases and hydrolases, used in the analysis of natural GAGs such as chondroitin sulfates, heparan sulfate, and keratan sulfates. We found that PPS did not interfere with GAG analysis, suggesting that a combination of chemical and enzymatic treatment could be used to analyze samples containing both natural GAGs and PPS.

Received 31st May 2019,
Accepted 1st July 2019

DOI: 10.1039/c9an01006h

rsc.li/analyst

Introduction

Glycosaminoglycans (GAGs) are a family of structurally complex heteropolysaccharides, populating the cell surface and extracellular matrix, which are biosynthesized in the Golgi or on the cell membrane.[1,2] GAGs are found as free glycans or attached to a core protein in the form of proteoglycans. They control a wide range of physiological and pathological events, such as cell–cell interactions, enzyme inhibition, cell proliferation, and growth factor receptor during various metabolic processes.[3–6] GAGs can be divided into four major classes based on their disaccharide repeating units (Fig. 1): heparan sulfate/heparin (HS/HP), chondroitin sulfate/dermatan sulfate (CS/DS), keratan sulfate (KS) and hyaluronan (HA). These units consist of an amino sugar, either *N*-acetyl-D-glucosamine (GlcNAc) or *N*-acetyl-D-galactosamine (GalNAc), and either an uronic acid, D-glucuronic (GlcA) or L-iduronic acid (IdoA), or galactose (Gal) in the case of KS.[2]

The most important structural determination of GAGs is disaccharide and oligosaccharide composition analysis because this provides information about the family to which it

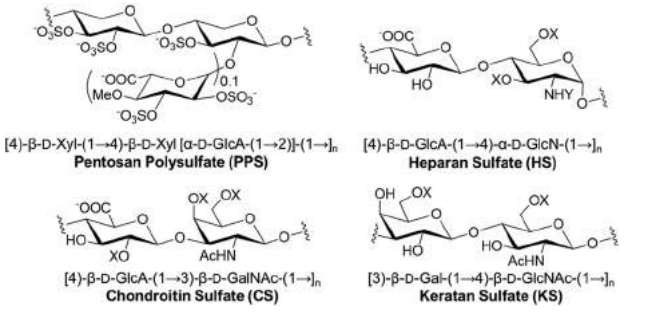

Fig. 1 Structures of PPS, HS, CS and KS. Group X is either H or SO_3^- and group Y is acetyl or SO_3^-. The primary carbohydrate backbone is shown below each structure.

[a]*School of Environment, Nanjing Normal University, Wenyuan Road 1, Nanjing 210023, China*
[b]*Department of Chemistry and Chemical Biology, Center for Biotechnology and Interdisciplinary Studies. Rensselaer Polytechnic Institute, Troy, New York, 12180, USA. E-mail: linhar@rpi.edu*
[c]*Department of Chemical and Biological Engineering, Center for Biotechnology and Interdisciplinary Studies, Rensselaer Polytechnic Institute, Troy, New York, 12180, USA*
[d]*School of Food Science and Pharmaceutical Engineering, Nanjing Normal University, Wenyuan Road 1, Nanjing 210023, China. E-mail: beishidazhangxing@163.com*
[e]*State Key Laboratory of Natural and Biomimetic Drugs, Peking University, Beijing, 100191, P R China*
† Equal contributors.

belongs and can be used in studying the pharmacokinetics of these polycomponent/polypharmacological drugs.[7] This method relies on the enzymatic depolymerization of GAG using polysaccharide lyases or hydrolases[8] and then measuring the resulting disaccharide and oligosaccharides by liquid chromatography mass spectrometry (LC-MS) in a bottom-up type of analysis.[9,10] Semi-synthetic GAGs such as oversulfated chondroitin sulfate, resistant to enzymatic break down, have been similarly subjected to bottom-up analysis by relying on reactive oxygen species (ROS), generated by chemical reagents and radiation, for their depolymerization.[11,12] These previous studies showed that ROS-based degradation did not preferentially cleave side chains or sulfo groups, and the primary structure of the molecules can be retained after degradation. Thus, ROS-based depolymerization were complementary with the enzymatic digestion, since it is relatively nonselective in fragmenting a wide variety of polysaccharides, even those resistant to enzymatic depolymerization.

Pentosan polysulfate (PPS) is a heparin mimetic with a highly sulfated polysaccharide backbone (Fig. 1). PPS is synthesized through the chemical sulfonation of a plant-derived β-(1 → 4)-xylan is the active pharmaceutical ingredient of a drug Elmiron™. This linear poly(xylan) backbone is occasionally (in a ratio of 1 uronic acid to 9 xylose units) substituted with 4-methyl glucopyranosyl uronic acid units glycosidically linked to the 2-position of the main chain. PPS shows multiple biological activities, including anti-inflammatory and anticoagulant activity. PPS has been used as an anti-thrombotic agent in clinic in the United States for the management of patients with interstitial cystitis.[13–16] Moreover, its multiple effects on coagulation, fibrinolysis, platelet functions and vascular cells have led to the study of PPS in a wide array of clinical disorders such as antagonism of enzymatic activities[17] (leukocyte elastase, protein kinases and reverse transcriptase) and inhibition of HIV infectivity.[18]

PPS has a molecular weight range of 4000 to 6000 Da, similar to that of low molecular weight heparins (LMWHs).[19] This suggested that direct structural profiling of PPS by top-down analysis might be useful in gaining a better understanding of this polycomponent/polypharmacological drug. Variations in the degree of sulfation, length of the oligosaccharide chain and glucuronosyl branching modifications might create complex mixtures containing hundreds or more different species of PPS.

Since PPS and GAGs are all widely used drugs in the treatment of human disease, and they are structurally similar they both would be depolymerized by ROS, suggesting that PPS and GAGs may interfere each other during analysis in complicated biological samples. However, to date, very few studies have investigated these issues. Here, we have developed a ROS-based depolymerization bottom-up strategy and systematically studied the feasibility of PPS quantification in the presence of GAGs. We also took advantage of the similarity of the molecular weight properties between PPS and LMWHs to apply a top-down LC-MS method for the direct analysis of PPS chains. Finally, a series of enzymatic degradation studies were performed on GAGs in the presence of PPS to test whether PPS inhibited GAG lyases. These studies provide a much clearer picture of how GAG analysis might be undertaken in the presence of the semi-synthetic GAG mimetic, PPS, and suggest approaches for the possible application in the analysis of more complex biological samples.

Results and discussion

Oxidative depolymerization of PPS was conducted by treatment with hydrogen peroxide and copper acetate, and then followed by quenching with sodium bisulfite. Hydrophilic interaction liquid chromatography (HILIC)-MS, which has been proved to be a powerful tool for low molecular weight heparin analysis, was utilized for the direct monitoring of ROS-treated PPS. As can be seen from Fig. 2A, direct analysis from HILIC-MS showed that the major component of oxidatively depolymerized PPS is the disulfated xylose monosaccharide. Di-, tri-, tetra-, and penta- saccharides of disulfated xylose contribute very small amounts of the oxidation products. High-resolution mass analysis also displayed that extracted ion chromatography of peak at m s^{-1} 308.9586 (Fig. 2B) corresponding to the $[M - H]^{1-}$ ion of disulfated xylose monosaccharide.

A possible mechanism for radical depolymerization of PPS is proposed in Fig. 3. In the ROS system, hydrogen peroxide is activated by copper (Cu^{2+}) ions to generate hydroxyl radicals ($HO^{\bullet}$) *via* complex reaction sequences [eqn (1) and (2)]. The unpaired electron of $HO^{\bullet}$ radicals make them strong oxidants, react with PPS and cause them to depolymerize.[20–22] Hydroxyl radicals generated by copper acetate and hydrogen peroxide can extract hydrogen, which in turn produces free radical species that can break the chain at the glycosidic bond.

The reaction crude was treated by gel filtration chromatography through a Bio-Gel P-2 column to further confirm the structure of the monosaccharide product. The purified product was analyzed by 1D and 2D NMR (Fig. 4). In the ^{1}H NMR spectrum, all the proton signals are assigned except H-3, which is overlapped with HOH^{2} peak but could be clearly observed as H-3/C-3 (4.71 ppm, 72.1 ppm) in ^{1}H–^{13}C HSQC spectrum, suggesting that there is a strong electron-withdraw-

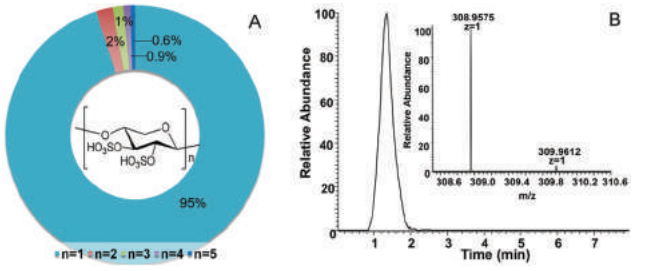

Fig. 2 (A) Major composition of ROS radical depolymerized PPS roughly calculated by peak area obtained from HILIC-MS analysis. (B) HILIC-MS extracted ion chromatogram (EIC) of peaks at *m/z* 308.9586 (±5 ppm). Insert: Spectrum of the isotopic peaks of *m/z* 308.9586, which corresponds to a disulfated xylose monosaccharide.

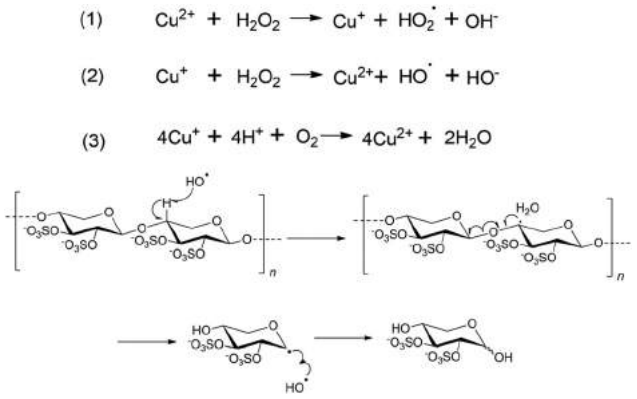

Fig. 3 Proposed mechanism for radical depolymerization of PPS.

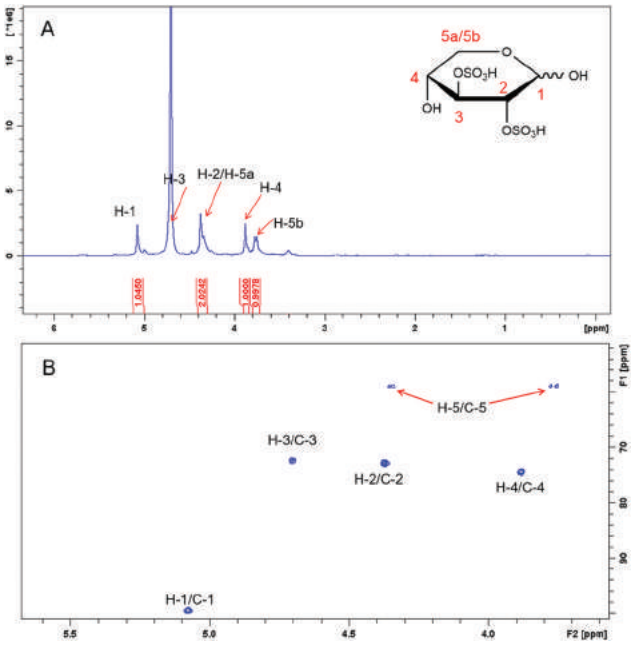

Fig. 4 (A) ^{1}H and (B) $^{1}H-^{13}C$ HSQC spectra of depolymerized monosaccharide.

ing sulfo group at position 3 of the sugar ring. Combining HSQC and COSY experiments, we were able to identify the proton signals of H-2 and H-4 were 4.36 and 3.87 ppm, which is consistent with the structure of the product, confirming that the depolymerized product is a monosaccharide xylose with two sulfate groups on the position of 2 and 3. This unique compound is completely different from any potential GAG depolymerization moiety, and so make the PPS analysis achievable in the presence of GAGs.

Two main factors that affected monosaccharide yield have been carefully investigated to improve our depolymerization strategy. Oxidation reaction time plays a crucial role in the free radical induced polysaccharide degradation. As shown in Fig. 5A, as the ROS reaction time increased, the peak area of the target monosaccharide gradually increased, and finally reached a plateau in 1 h, indicating a tendency to complete

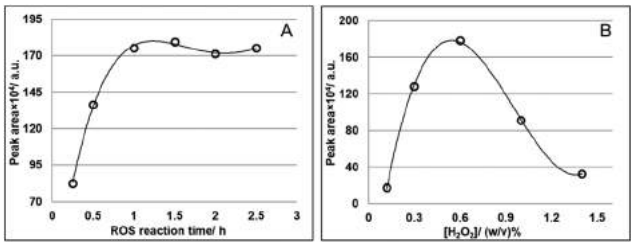

Fig. 5 Optimization of (A) ROS reaction time and (B) H_2O_2 concentration.

the cleavage process. Accordingly, the optimal reaction time was chosen to be 1 h. H_2O_2 provides hydroxyl radicals and its amount has a strong influence on the efficiency of depolymerization process. Fig. 5B demonstrates that the peak area of the target monosaccharide increased with the growing H_2O_2 concentration. The signal value reached its maximum at the H_2O_2 concentration of 0.6% (w/v), while started to decrease when the H_2O_2 concentration further increased. The reducing signal response implied the undesirable monosaccharide degradation at higher H_2O_2 concentration. This phenomenon stems from the factor that excess addition of H_2O_2 could lead to higher H^+ concentration in the system. The reaction between Cu^+ and H_2O_2 [eqn (1)] is severely inhibited by molecular oxygen since Cu^+ is quantitatively oxidized by oxygen to Cu^{2+} in acidic conditions [eqn (3)]. Therefore, the effective [Cu^+] that can react with H_2O_2 was significantly decreased and the depolymerization efficiency was also reduced. Thus, H_2O_2 concentration was optimized to be 0.6% (w/v).

For the sake of evaluating the method feasibility of PPS analysis, different concentration of PPS were treated by ROS depolymerization and then tested by HILIC-MS in the presence of other GAGs. The EICs of disulfated xylose monosaccharides at different PPS concentration on the optimal assay conditions is shown in Fig. 6A. Signal intensity gradually increased as the concentration of PPS varied from 1 to 50 ng μL^{-1}. The dependence of monosaccharide peak area on PPS concentration is presented in Fig. 6B. The fluorescence signal was linearly increased with the PPS concentration in the range from 1 to 50 ng μL^{-1}. The linear relationship can be described as $y = 3.51x + 5.07$ with the correlation coefficient of $r^2 = 0.988$, where y is

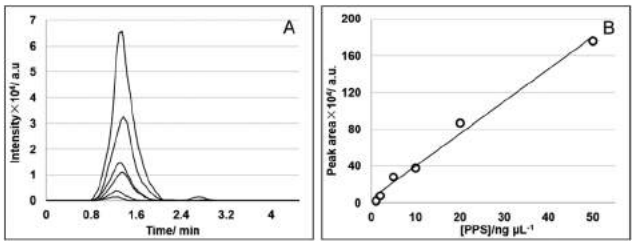

Fig. 6 (A) EICs of bisulfated monosaccharides at different PPS concentration (bottom to top, 1, 2, 5, 10, 20, 50 ng μL^{-1}) in the presence of 100 ng μL^{-1} GAG mixture. (B) Dependence of monosaccharide peak area on PPS concentration.

the peak area of disulfated monosaccharide and x is the PPS concentration. This demonstrates that our proposed method can be applied to PPS analysis in a wide concentration range without interference by high concentrations of GAGs.

A top-down approach was next applied for the analysis of intact PPS chains providing a structural profile. This top-down method utilizes a simple and reliable HILIC-FT-ESI-MS platform to characterize marketed PPS products and require no special sample preparation steps. In the identification of PPS components, a theoretical database was generated by GlycReSoft 1.0 using the following parameters: A. Xylose = 2–20; B. SO_3 = A–2A; C. 4-Methyglucuronic acid = 0–5. The statistical profiling results are presented in Fig. 7. The total ion chromatography (TIC) was obtained and a mass spectrum of each peak was obtained. For example, the peak at 14.38 min shows a mass of 445.933 with a −2 charge (z) representing an isotopic mass of 893.882. Using GlycoReSoft and GlycCompSoft[23] software, we can assign the peak corresponding to the [3, 6, 0], where 3 represents the number xylose and 6 represents the number of sulfate groups. PPS showed 54 identifiable peaks ranging from [3, 5, 0] with 3 xylose and 5 sulfates to [20, 25, 2] with 20 xylose, 25 sulfates and two 4-methyglucuronic acid. The samples were analyzed in triplicate and the standard deviation was analytical error.

Enzyme specificity is one of the most important aspects in GAG analysis. We further investigated whether PPS inhibited typical enzymes used during GAGs analysis, including heparinase, chondroitinase and keratanse (Fig. 8). HS, CS and KS were treated with specific enzyme and then analyzed by LC-MS/MS, respectively. Control experiments were conducted with interferences containing 100 ng μL^{-1} PPS, which was 10 times higher than GAG concentration. Disaccharide compositional analysis of GAG with and without PPS are shown in Fig. 8A–C. No significant variation was observed in different disaccharide components even when PPS up to 100 ng μL^{-1} was applied. PPS also shows no effect on total GAG analysis (Fig. 8D). This result is consistent with the high specificities of heparinase, chondroitinase and keratanse for HS, CS and KS, respectively, and suggest the feasibility of accurate GAG analysis in the presence of high concentration of PPS.

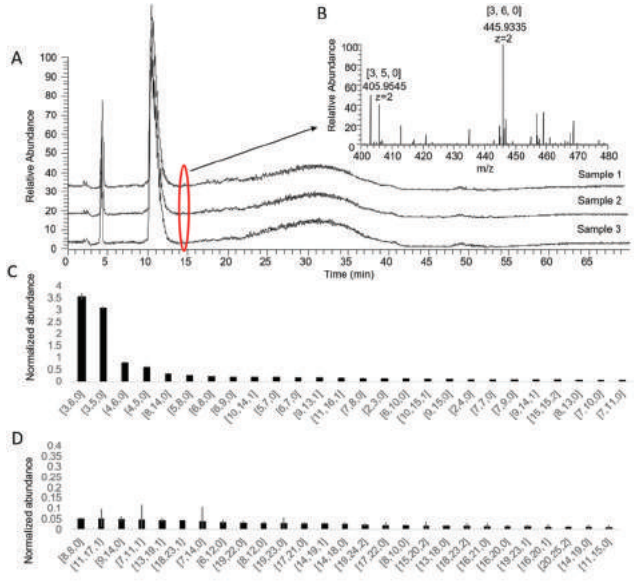

Fig. 7 Quantitative analysis of identified intact PPS chains. (A) TIC of three PPS samples peaks at 4 and 11 min are salts and the peaks from 14 min to 40 min are PPS chains. The small peak circled at 14.66 min corresponds to the trisaccharide fraction. (B) MS of retention time of this trisaccharide peak were assigned to two major components [3, 6, 0] and [3, 5, 0]. Other fractions from the TIC were analyzed by MS, identified and used to construct panels (C) and (D). Normalized abundance of identified components. Oligosaccharide compositions are given as [xylose, SO_3, 4-methyglucuronic acid].

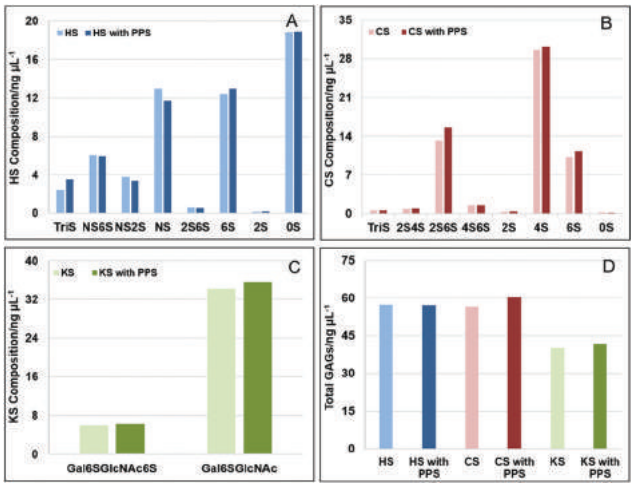

Fig. 8 The disaccharide composition of (A) HS, (B) CS, (C) KS and (D) total GAG analysis with and without the presence of PPS.

Experimental

Materials

Unsaturated disaccharide standards of CS ($0S_{CS\text{-}0}$: ΔUA-GalNAc; $4S_{CS\text{-}A}$: ΔUA-GalNAc4S; $6S_{CS\text{-}C}$: ΔUA-GalNAc6S; $2S_{CS}$: ΔUA2S-GalNAc; $2S4S_{CS\text{-}B}$: ΔUA2S-Gal-NAc4S; $2S6S_{CS\text{-}D}$: ΔUA2S-GalNAc6S; $4S6S_{CS\text{-}E}$: ΔUA-GalNAc4S6S; $TriS_{CS}$: ΔUA2S-GalNAc4S6S), unsaturated disaccharide standards of HS ($0S_{HS}$: ΔUA-GlcNAc; NS_{HS}: ΔUA-GlcNS; $6S_{HS}$: ΔUA-GlcNAc6S; $2S_{HS}$: ΔUA2S-GlcNAc; $2SNS_{HS}$: ΔUA2S-GlcNS; $NS6S_{HS}$: ΔUA-GlcNS6S; $2S6S_{HS}$: ΔUA2S-GlcNAc6S; $TriS_{HS}$: ΔUA2S-GlcNS6S), were purchased from Iduron (UK), where ΔUA is 4-deoxy-α-L-*threo*-hex-4-enopyranosyluronic acid. Pentosan polysulfate (PPS), 2-aminoacridone (AMAC), sodium cyanoborohydride ($NaCNBH_4$), hydrogen peroxide, copper acetate, and acetic acid were purchased from Sigma-Aldrich (St Louis, MO). Methanol (HPLC grade), ammonium acetate (HPLC grade), acetonitrile (HPLC grade), and dimethyl sulfoxide (DMSO) were purchased from Fisher Scientific (Springfield, NJ). *E. coli* expression and purification of the recombinant *F. heparinum* heparin lyase I, II, III (EC No.

4.2.2.7, 4.2.2.X, and 4.2.2.8, respectively) and *P. vulgaris* chondroitin lyase ABC (EC No. 4.2.2.20) were performed in our laboratory as described.[24] Bio-Gel P-2 Gel (fine polyacrylamide beads for size exclusion chromatography, 45–90 μm wet bead size, 100–1800 MW fractionation range) was purchased from Bio-Rad Laboratories, Inc.

Depolymerization of PPS

PPS samples were dissolved in 100 μL 0.1 M sodium acetate-acetic acid solution containing 0.2 mM copper(II) acetate and adjusted to pH 7.0. Hydrogen peroxide (2 μL of 30% solution) was added with mixing and reacted at 45 °C for 1 h. Sodium bisulfite was added to terminate the reaction by removing excess unreacted hydrogen peroxide. The reaction mixture was lyophilized and finally re-dispersed in 100 μL H_2O for LC-MS analysis. GAG (100 ng μL^{-1}) and PPS mixture was used as controlled samples and treated the same way.

LC-MS analysis using a Luna HILIC column (2.0 × 50 mm, 200 Å, Phenomenex, Torrance, CA, USA) connected online to the standard electrospray ionization (ESI) source of an LTQ Orbitrap XL FT-MS instrument (Thermo Fisher Scientific, San Jose, CA, USA). Gradient elution used 3 to 50% 5 mM aqueous ammonium acetate with 97 to 50% 5 mM aqueous ammonium acetate in 98% acetonitrile over 7 min at 250 μl min^{-1}. The optimized parameters, used to prevent in-source fragmentation, included a spray voltage of 4.2 kV, a capillary voltage of −40 V, a tube lens voltage of −50 V, a capillary temperature of 275 °C, a sheath flow rate of 30, and an auxiliary gas flow rate of 6. External calibration of mass spectra routinely produced a mass accuracy of better than 3 ppm. All FT mass spectra were acquired at a resolution 30 000 with 300–2000 Da mass range.

1D and 2D NMR analyses

All samples were dissolved in 400 μL of ^2H_2O (99.9 atom %) and lyophilized three-times to remove the exchangeable protons. The samples were dissolved in 400 μL of ^2H_2O (99.96% atom %) and transferred to NMR microtubes. All NMR experiments were performed at 273 K on Bruker Advance II 600 MHz with Topspin 2.1.6 software. One-dimensional ^1H spectra were recorded for 32 scans and an acquisition time of 850 ms. 2D ^1H–^{13}C HSQC experiments were performed with 24 scans, 1.5 s relaxation delay, and 400 ms acquisition time.

Structural profiling of PPS by HILIC-MS

PPS samples were prepared at concentration of 10 μg μL^{-1}. A Luna HILIC column (2.0 × 150 mm, 200 Å, Phenomenex, Torrance, CA) was used to separate the intact chains. Mobile phase A was 5 mM ammonium acetate prepared with HPLC grade water. Mobile phase B was 5 mM ammonium acetate prepared in 98% HPLC grade acetonitrile with 2% of HPLC grade water. HPLC binary pump was used to deliver the gradient from 10% A to 35% A over 40 min at a flow rate of 150 μL min^{-1}. The source parameters for FTMS detection were optimized to minimize the in-source fragmentation and sulfate loss and maximize the signal/noise in the negative-ion mode. The optimized parameters, used to prevent in-source fragmentation, included a spray voltage of 4.2 kV, a capillary voltage of −40 V, a tube lens voltage of −50 V, a capillary temperature of 275 °C, a sheath flow rate of 30 L min^{-1}, and an auxiliary gas flow rate of 6 L min^{-1}. All FT mass spectra were acquired at a resolution 60 000 with 200–2000 Da mass range. Raw spectral data are available upon request.

Disaccharide analysis of GAG samples

HS, CS, and KS samples were dissolved in 300 μL of digestion buffer (50 mM ammonium acetate, 2 mM calcium chloride) and treated with recombinant heparin lyase (I, II, III), chondroitin lyase ABC and keratanase (I, II) (10 mU each), respectively. The reaction mixture was placed in 37 °C incubator for 2 h and then terminated by eliminating enzyme *via* passing through 3 kDa MWCO spin columns. The filter unit was washed twice with 200 μL of distilled water and the filtrate was finally lyophilized. GAG and PPS (100 ng μL^{-1}) mixture was used as controlled samples and treated the same way.

The dried samples were AMAC-labeled by adding 10 μL of 0.1 M AMAC in DMSO/acetic acid (17/3, V/V) incubating at room temperature for 10 min, followed by adding 10 μL of 1 M aqueous $NaBH_3CN$ and incubating for 1 h at 45 °C. The resulting samples were centrifuged at 13 200 rpm for 10 min. Finally, each supernatant was collected and stored in a light resistant container at room temperature until analyzed *via* LC-MS/MS. LC was performed on an Agilent 1200 LC system at 45 °C using an Agilent Poroshell 120 ECC18 (2.7 μm, 3.0 × 50 mm) column. Mobile phase A (MPA) was 50 mM ammonium acetate aqueous solution, and the mobile phase B (MPB) was methanol. The mobile phase passed through the column at a flow rate of 300 μL min^{-1}. The gradient was 0–10 min, 5–45% B; 10–10.2 min, 45–100% B; 10.2–14 min, 100% B; 14–22 min, 100–5% B. A triple quadrupole mass spectrometry system equipped with an ESI source (Thermo Fisher Scientific, San Jose, CA) was used a detector. The online MS analysis was at the Multiple Reaction Monitoring (MRM) mode. MS parameters: negative ionization mode with a spray voltage of 3000 V, a vaporizer temperature of 300 °C, and a capillary temperature of 270 °C.

Conclusions

In summary, we have developed a ROS-based depolymerization bottom-up strategy and systematically studied the feasibility of PPS quantification in the presence of GAGs. A top-down LC-MS method was applied for the direct analysis of PPS chains. HILIC-MS provides only a relative distribution of chains useful in the comparisons of different PPS products or batches and cannot be used to determine a products molecular weight distribution. Enzymatic degradation study of GAGs and PPS mixtures was also investigated and results showed that there was no inhibition effect of PPS on heparinase, chondroitinase and keratanase. This work not only addressed the concern of interference between PPS and GAGs,

but also paved the way for more complicated GAGs analysis in biological samples that coexists with PPS.

Conflicts of interest

There are no conflicts to declare.

Acknowledgements

This work was supported by grants from the National Institutes of Health DK 111958, CA 231074 and Open Project Program of the State Key Laboratory of Natural and Biomimetic Drugs K20190203.

References

1 U. Lindahl, J. Couchman, K. Kimata and J. D. Esko, *Essentials of Glycobiology*, ed. R. D. Cummings, A. Varki, J. D. Esko, P. Stanley, G. W. Hart, A. G. Darvill, M. Aebi, T. Kinoshita, N. H. Packer, J. H. Prestegard, R. L. Schnaar and P. H. Seeberger, Cold Spring Harbor, Laboratory Press CSHN, 3rd edn, 2017, 2015–2017, ch. 17.
2 P. L. DeAngelis, J. Liu and R. J. Linhardt, *Glycobiology*, 2013, **23**, 764–777.
3 D. Xu and J. D. Esko, *Annu. Rev. Biochem.*, 2014, **83**, 129–157.
4 I. Capila and R. J. Linhardt, *Angew. Chem., Int. Ed.*, 2002, **41**, 390–412.
5 R. J. Linhardt and T. Toida, *Acc. Chem. Res.*, 2004, **37**, 431–438.
6 S. Mizumoto, S. Yamada and K. Sugahara, *Curr. Opin. Struct. Biol.*, 2015, **34**, 35–42.
7 G. Li, J. Steppich, Z. Wang, Y. Sun, C. Xue, R. J. Linhardt and L. Li, *Anal. Chem.*, 2014, **86**, 6626–6632.
8 X. Zhang, K. Xia, L. Lin, F. Zhang, Y. Yu, K. St. Ange, X. Han, E. Edsinger, J. Sohn and R. J. Linhardt, *ACS Chem. Biol.*, 2018, **13**, 1677–1685.
9 S. Y. Kim, C. A. Koetzner, A. F. Payne, G. J. Nierode, Y. Yu, R. Wang, E. Barr, J. S. Dordick, L. D. Kramer, F. Zhang and R. J. Linhardt, *Biochemistry*, 2019, **58**, 1155–1166.
10 Y. Yu, F. Zhang, W. Colón, R. J. Linhardt and K. Xia, *Anal. Biochem.*, 2018, **567**, 82–84.
11 G. Li, C. Cai, L. Li, L. Fu, Y. Chang, F. Zhang, T. Toida, C. Xue and R. J. Linhardt, *Anal. Chem.*, 2014, **86**, 326–330.
12 X. Zhao, B. Yang, L. Li, F. Zhang and R. J. Linhardt, *Carbohydr. Polym.*, 2013, **96**, 503–509.
13 J. P. Maffrand, J. M. Herbert, A. Bernat, G. Defreyn, D. Delebassee, P. Savi, J. J. Pinot and J. Sampol, *Semin. Thromb. Hemostasis*, 1991, **17**, 186–198.
14 K. S. Kilgore, K. B. Naylor, E. J. Tanhehco, J. L. Park, E. A. Booth, R. A. Washington and B. R. Lucchesi, *J. Pharmacol. Exp. Ther.*, 1998, **285**, 987–994.
15 L. J. Herrero, S. S. Foo, K. C. Sheng, W. Chen, M. R. Forwood, R. Bucala and S. Mahalingam, *J. Virol.*, 2015, **89**, 8063–8076.
16 C. L. Parsons, G. Benson, S. J. Childs, P. Hanno, G. Sant and G. Webster, *J. Urol.*, 1993, **160**, 845–848.
17 G. Sydow and H. P. Klocking, *Biochim. Biophys. Acta*, 1987, **46**, 527–530.
18 M. Baba, M. Nakajima, D. Schols, R. Pauwels, J. Balzarini and E. De Clercq, *Antiviral Res.*, 1988, **9**, 335–343.
19 X. Liu, K. St. Ange, L. Lin, F. Zhang, L. Chi and R. J. Linhardt, *J. Chromatogr. A*, 2017, **1480**, 32–40.
20 J. Li, S. Li, S. Liu, C. Wei, L. Yan, T. Ding, R. J. Linhardt, D. Liu, X. Ye and S. Chen, *Int. J. Biol. Macromol.*, 2019, **124**, 1025–1032.
21 Z. Zhi, J. Chen, S. Li, W. Wang, R. Huang, D. Liu, T. Ding, R. J. Linhardt, S. Chen and X. Ye, *Sci. Rep.*, 2017, **7**, 541.
22 A. D. Bokare and W. J. Choi, *Hazard. Mater.*, 2014, **275**, 121–135.
23 X. Wang, X. Liu, L. Li, F. Zhang, M. Hu, F. Ren, L. Chi and R. J. Linhardt, *PLoS One*, 2016, **11**, e0167727.
24 H. Su, F. Blain, R. A. Musil, J. J. Zimmermann, K. Gu and D. C. Bennett, *Appl. Environ. Microbiol.*, 1996, **62**, 2723–2734.